

# Control of enhanced THz transmission through metallic hole arrays using nematic liquid crystal

Ci-Ling Pan

*Department of Photonics and Institute of Electro-Optical Engineering  
National Chiao Tung University, Hsinchu, Taiwan 30010, R.O.C.  
[clpan@faculty.nctu.edu.tw](mailto:clpan@faculty.nctu.edu.tw)*

Cho-Fan Hsieh, and Ru-Pin Pan

*Department of Electrophysics  
National Chiao Tung University, Hsinchu, Taiwan 30010, R.O.C.  
[rpchao@mail.nctu.edu.tw](mailto:rpchao@mail.nctu.edu.tw)*

Masaki Tanaka, Fumiaki Miyamaru, Masahiko Tani, and Masanori Hangyo

*Institute of Laser Engineering, Osaka University,  
Yamadaoka 2-6, Suita, Osaka 565-0871, Japan*

**Abstract:** We demonstrate frequency tuning of enhanced THz radiation transmitted through a two-dimensional metallic hole array (2D-MHA) by controlling the index of refraction of the medium filling the holes and adjacent to the 2D-MHA on one side. The medium is a nematic liquid crystal (NLC) and its index of refraction is varied using magnetically controlled birefringence of the NLC. With the NLC, the peak transmission frequency of the 2D-MHA shift to the red by 0.112 THz and can be tuned from 0.193 to 0.188 THz. The peak transmittance is as high as 70% or an enhancement of 2.42 times, considering the porosity of the 2D-MHA. As a tunable THz filter, this device exhibits a continuous tuning range of 4.7 GHz, a low insertion loss of 2.35 to 1.55 dB and a quality factor of ~ 4-5.

©2005 Optical Society of America

**OCIS codes:** (050.1220) apertures, (050.0050) Diffraction and gratings, (120.2440) Filters, (230.3720) Liquid-crystal devices, (240.6680) Surface plasmons, (260.3090) Infrared, far, (320.0320) Ultrafast optics, and THz

---

## References and links

1. T. W. Ebbesen, H. J. Lezec, H. F. Ghaemi, T. Thio, and P. A. Wolff, "Extraordinary optical transmission through sub-wavelength hole arrays," *Nature (London)* **351**, 667, 1998.
2. H. F. Ghaemi, T. Thio, D. E. Grupp, T. W. Ebbesen, and H. J. Lezec, "Surface plasmons enhance optical transmission through subwavelength holes," *Phys. Rev. B* **58**, 6779 (1998).
3. E. Popov, M. Nevière, S. Enoch, and R. Reinisc, "Theory of light transmission through subwavelength periodic hole arrays," *Phys. Rev. B* **62**, 16100 (2000).
4. W. L. Barnes, A. Dereux, and T. W. Ebbesen, "Surface plasmon subwavelength optics," *Nature (London)* **424**, 824 (2003).
5. D. E. Grupp, H. J. Lezec, T. W. Ebbesen, K. M. Pellerin and T. Thio, "Crucial role of metal surface in enhanced transmission through subwavelength apertures," *Appl. Phys. Lett.* **77**, 1569 (2000).
6. A. Krishnan, T. Thio, T. J. Kim, H. J. Lezec, T. W. Ebbesen, P. A. Wolff, J. B. Pendry, L. Martín-Moreno, and F. J. García-Vidal, "Evanescently coupled resonance in surface plasmon enhanced transmission," *Opt. Commun.* **200**, 1 (2001).
7. L. Martín-Moreno, F. J. García-Vidal, H. J. Lezec, K. M. Pellerin, T. Thio, J. B. Pendry, and T. W. Ebbesen, "Theory of Extraordinary Optical Transmission through Subwavelength Hole Arrays," *Phys. Rev. Lett.* **86**, 1114 (2001).
8. H. Raether, *Surface Plasmons on Smooth and Rough Surfaces and on Gratings* (Springer-Verlag, Berlin, 1988).
9. T. Thio, H. F. Ghaemi, H. J. Lezec, P. A. Wolff, and T. W. Ebbesen, "Surface-plasmon-enhanced transmission through hole arrays in Cr films," *J. Opt. Soc. Am. B* **16**, 1743 (1999).

10. A. Degiron, H. J. Lezec, W. L. Barnes, T. W. Ebbesen, "Effects of hole depth on enhanced light transmission through subwavelength hole arrays," *Appl. Phys. Lett.* **81**, 4327 (2002).
11. T. J. Kim, T. Thio, T. W. Ebbesen, D. E. Grupp, and H. J. Lezec, "Control of optical transmission through metals perforated with subwavelength hole arrays," *Opt. Lett.* **24**, 256 (1999).
12. T. K. Wu, *Frequency Selective Surface and Grid Array* (Wiley, New York, 1995).
13. C. Winnewisser, F. T. Lewen, M. Schall, M. Walther, and H. Helm, *IEEE Trans. "Characterization and Application of Dichroic Filters in the 0.1–3-THz Region," Microwave Theory Tech.* **48**, 744 (2000).
14. H. Cao and A. Nahata, "Resonantly enhanced transmission of terahertz radiation through a periodic array of subwavelength apertures," *Opt. Express* **12**, 1004 (2004).  
<http://www.opticsexpress.org/abstract.cfm?URI=OPEX-12-6-1004>
15. D. Qu, D. Grischkowsky, and W. Zhang, "Terahertz transmission properties of thin, subwavelength metallic hole arrays," *Opt. Lett.* **29**, 896 (2004).
16. J. Gómez Rivas, C. Schotsch, P. Haring Bolivar, and H. Kurz, "Enhanced transmission of THz radiation through subwavelength holes," *Phys. Rev. B* **68**, 201306 (2004).
17. L. Martin-Moreno, F. Garcia-Vidal, H. Lezec, A. Degiron, and T. Ebbesen, "Theory of Highly Directional Emission from a Single Subwavelength Aperture Surrounded by Surface Corrugations," *Phys. Rev. Lett.* **90**, 167401 (2003).
18. J. B. Pendry, L. Martin-Moreno, F. J. Garcia-Vidal, "Mimicking Surface Plasmons with Structured Surfaces," *Science*, **305**, 847 (2004).
19. F. Miyamaru and M. Hangyo, "Anomalous terahertz transmission through double-layer metal hole arrays by coupling of surface plasmon polaritons," *Phys. Rev. B* **71**, 165408 (2005).
20. J. Gómez Rivas, P. Haring Bolivar, H. Kurz, "Thermal switching of the enhanced transmission of terahertz radiation through subwavelength apertures," *Opt. Lett.* **29**, 1680 (2004).
21. T. D. Drysdale, I. S. Gregory, C. Baker, E. H. Linfield, W. R. Tribe, D. R. S. Cumming, "Transmittance of a tunable filter at terahertz frequencies," *Appl. Phys. Lett.* **85**, 5173 (2004).
22. H. Némec, P. Kužel, L. Duvillaret, A. Pashkin, M. Dressel, M. T. Sebastin, "Highly tunable photonic crystal filter for the terahertz range," *Opt. Lett.* **30**, 549 (2005).
23. Tsong-Ru Tsai, Chao-Yuan Chen, Ci-Ling Pan, Ru-Pin Pan, and Xi Cheng Zhang, "Terahertz time-domain spectroscopy studies of the optical constants of the nematic liquid crystal 5CB," *Appl. Opt.* **42**, 2372, 2003.
24. Ru-Pin Pan, Tsong-Ru Tsai, Chiunghan Wang, Chao-Yuan Chen, and Ci-Ling Pan, "The Refractive Indices of Nematic Liquid Crystal 4'-n-pentyl-4-cyanobiphenyl in the THz Frequency Range," *Mol. Cryst. Liq. Crystl.*, 409 (2004).
25. Chao-Yuan Chen, Tsong-Ru Tsai, Ci-Ling Pan, and Ru-Pin Pan, "Room temperature terahertz phase shifter based on magnetically controlled birefringence in liquid crystals," *Appl. Phys. Lett.* **83**, 4497, 2003.
26. Chao-Yuan Chen, Cho-Fan Hsieh, Yea-Feng Lin, Ru-Pin Pan, and Ci-Ling Pan, "Magnetically tunable room-temperature  $2\pi$  liquid crystal terahertz phase shifter," *Opt. Express*, **12**, 2625 (2004).  
<http://www.opticsexpress.org/abstract.cfm?URI=OPEX-12-12-2625>
27. S. Nashima, O. Morikawa, K. Takata, and M. Hangyo, *J. Appl.* "Temperature dependence of optical and electronic properties of moderately doped silicon at terahertz frequencies," *J. Appl. Phys.* **90**, 837 (2001).
28. F. Miyamaru, M. Hangyo, "Finite size effect of transmission property for metal hole arrays in subterahertz region," *Appl. Phys. Lett.* **84**, 2742 (2004).
29. Masaki Tanaka, Fumiaki Miyamaru, Masanori Hangyo, Takeshi Tanaka, Masamichi Akazawa and Eiichi Sano, "Effect of thin dielectric layer on terahertz transmission characteristics for metal hole arrays," *Opt Lett.*, to be published. 2005.
30. C. Weil, S. Muller, R. Scheele, P. Best, g. Lussem, R. Jakoby, *Electron.* "Highly-anisotropic liquid-crystal mixtures for tunable microwave devices," *Electron. Lett.* **39**, 1732 (2003).

## 1. Introduction

Metal films with two-dimensional periodic arrays of subwavelength holes (2D-MHA) or metallic photonic crystals (2D-MPC), can exhibit extraordinary optical transmission characteristics [1-3]. This discovery attracts much attention because of its potential applications for subwavelength optics, data storage, microscopy and biophotonics [4]. Extensive work on the mechanism of the extraordinary transmission has been carried out both theoretically and experimentally [2, 5-7]. The enhanced transmission is now understood to be due to the resonant coupling of incident light with surface plasmon polaritons (SPPs) [8]. The SPP enhancement is observed in the case where no propagation mode is supported in the metal hole and the transmission peak frequency depends on the geometry of the structure [9], the angle of incidence of the radiation [1,2], depth of the holes [10], and can be tuned by the refractive index of the adjacent medium [5-7,9,11]. The tunability of extraordinary

transmission might lead to applications such as brighter flat-panel displays, spatial light modulators and tunable optical filters [2,11].

In the millimeter wave and terahertz (THz) regions, a 2D-MHA acts as a band-pass filter or frequency selective surface [12,13]. The band-pass peak frequency is above the cutoff frequency of the hole in this case. For such band-pass filters, the transmittance is several times larger than the porosity of the holes, and hence such transmission characteristics can also be called extraordinary transmission similar to that observed at optical wavelengths [1]. Very recently, enhanced THz transmission has been reported for subwavelength hole arrays in metal films [14,15] and doped semiconductor plates [16]. These advances are significant as they could lead to the realization of efficient THz sub-wavelength optics for ultra-sensitive THz sensing and imaging systems. The large permittivity of metals at lower than optical frequencies was believed to be a limitation for the scalability of the enhanced transmission phenomenon due to the resonant coupling of incident electromagnetic waves with SPP's [17]. As pointed out by Martin-Moreno *et al.* [17], however, the corrugation of the surface can give rise to an effective impedance or permittivity for surface modes. This favors the establishment of SPP's and enables enhanced transmission through metallic grating-like structures across an extended part of the electromagnetic spectrum. Recently, a new theory on the SPP-like mode on a structured perfect conductor metal has been proposed by Pendry *et al.* [18] The decay length of the SPP in the air side is infinitely large on the smooth perfect conductor, which means that the SPP is no more the "surface mode". However, the arrayed sub-wavelength holes make the surface "soft". That is, electromagnetic waves can partially penetrate the surface and the decay length in the dielectric side becomes finite. This is also confirmed in the simulation results of Miyamaru and Hangyo [19]. Strong localization of the THz wave is recognized and the extinction or attenuation length is on the order of the wavelength of the incident THz wave even though the perfect conductor is used.

Control of THz emission through the 2D-MHA is also expected to add new functionalities to future THz photonic crystal devices. Rivas *et al.* [20] demonstrated thermal switching of the THz transmission by modifying the density of free carriers in a silicon grating. The transmission peak of the 2D-MHA, however, can not be tuned in this way because the carrier density in metals does not change with temperature. A metallic photonic crystal was made tunable over the range of 365-386 GHz by a relative lateral shift of 140  $\mu\text{m}$  between two micromachined metallic photonic crystal plates [21]. The insertion loss and Q of the device are 3-7 dB and 20-30, respectively. By use of  $\text{SrTiO}_3$  as a defect material inserted into a periodic structure of alternating layers of quartz and high-permittivity ceramic, Nemeč *et al.* [22] was able to tune a single defect mode in the 1D photonic crystal from 185 GHz at room temperature down to 100 GHz at 100 K by thermal tuning. The peak transmittance exceeds -9 dB. In the near IR, Kim *et al.* [11] modulated the transmission amplitude (by 25%) of a perforated metal film-liquid crystal-indium tin oxide cell by varying the voltage applied to the LC. The spectral shift in the data is not immediately apparent, however, because the spectral features were quite broad in that experiment.

For a perfect metal, the transmission spectrum of the 2D-MHA with a triangular lattice of circular holes in the far-infrared is mainly characterized by several characteristic frequencies; the cutoff frequency of the  $\text{TE}_{11}$  mode,  $\nu_c = 1.841c/\pi d$ , where  $c$  is the speed of light in the holes and  $d$  is the diameter of the hole; the diffraction frequency,  $\nu_{\text{diff}} = 2c'/\sqrt{3}s$ , where  $c'$  is the speed of light in the medium adjacent to the metal surface,  $s$  is the lattice constant; and the resonant frequency of the SPP on a structured surface due to coupling of between electromagnetic radiation incident on a grating and the SPP [2],

$$\nu_R = \nu_{\text{spp}} = \left| \vec{k}_m + \vec{G} \right| \frac{c_o}{2\pi} \sqrt{\frac{\epsilon_m + \epsilon_d}{\epsilon_m \epsilon_d}}, \quad (1)$$

where  $\vec{k}_m$  is the in-plane wave vector component of the incident THz wave,  $c_o$  is the speed of light in vacuum,  $\vec{G}$  is the reciprocal lattice vectors of the periodic structure,  $\epsilon_m$  and  $\epsilon_d$  are the

dielectric constants of the metal and the adjacent dielectric medium, respectively;  $V_c$  determines the lower frequency limit below which electromagnetic waves become evanescent in the metallic circular hole. The diffraction frequency determines the lowest frequency above which electromagnetic waves are diffracted into the first diffraction lobe. The transmission peak frequency of the 2D-MHA almost coincides with the resonant frequency of the SPP on a smooth surface. For THz waves propagating through the 2D-MHA,  $|\epsilon_m| \gg \epsilon_d$ , the peak or resonant transmission frequency of the 2D-MHA,

$$V_R = V_{spp} \cong \frac{V_{diff}}{n_d}, \quad (2)$$

where  $v_{spp}$  is the surface plasmon-polariton (SPP) resonance frequency in the absence of the dielectric and  $n_d = \sqrt{\epsilon_d}$ , where  $n_d$  is the index of refraction of the dielectric. It is then possible to tune the SPP resonance frequency monotonically by varying  $n_d$ .

We have recently shown that the 4'-n-pentyl-4-cyanobiphenyl or 5CB, a nematic liquid crystal (LC), exhibits large birefringence and negligible absorption in the THz frequency range [23,24]. A liquid crystal THz phase shifter with magnetically-tunable phase shift [25] exceeding  $2\pi$  at 1 THz was realized [26]. In this letter, we demonstrate frequency tuning of enhanced THz radiation transmitted through a 2D-MHA by controlling the index of refraction of 5CB filling the holes and adjacent to the 2D-MHA on one side.

## 2. Experimental methods

The 2D-MHA was a 0.5 mm-thick aluminum plate perforated with circular holes arrayed in a triangular lattice of lattice constant  $s = 0.99$  mm and the diameter of each hole,  $d = 0.56$  mm. The 2D-MHA was machined on the one side and sandwiched by a pair of Mylar sheets (75  $\mu\text{m}$  in thickness) so that a box-like structure of dimension,  $0.15 \times 15.0 \times 15.0$  mm<sup>3</sup>, in the center of the 2D-MHA is formed for holding the LC (5CB, Aldrich, 98% purity). The holes of the MHA are also filled with LC material. A pair of rotatable permanent magnets is used to align the LC molecules as shown in Fig. 1.

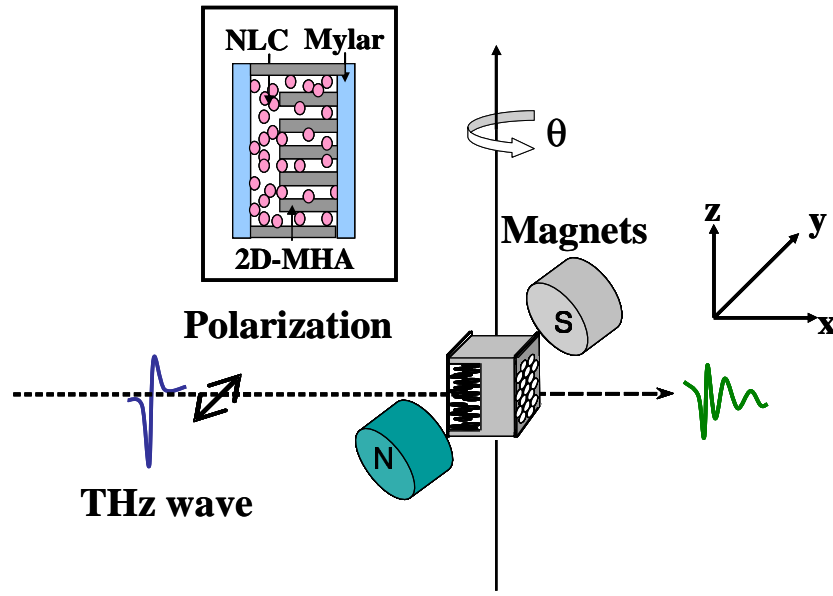


Fig.1. Experimental setup. The inset shows construction of the 2D-MHA with a nematic liquid crystal, (NLC) 5CB infiltrated and as the substrate on one side.

The magnetic field at the center on the sample cell is 0.15 T, which is much larger than the critical field ( $\sim 0.05$  T) required for aligning the LC molecules to the field [25]. The LC cell is otherwise not aligned by any other means. By rotating the magnet assembly about the z-axis at an angle  $\theta$  with respect to the sample plane (yz-plane in Fig. 1), the effective refractive index,  $n_d$ , of the LC infiltrated in and on one side of the 2D-MHA is changed from extra-ordinary refractive index,  $n_e = 1.75$  to ordinary refractive index,  $n_o = 1.57$ . Since the magnetic field is significantly larger than the threshold field to re-orient the LC molecules, the effective refractive index of LC can be written as

$$n_d = \left\{ \left[ \frac{\sin^2(\theta)}{n_o^2} + \frac{\cos^2(\theta)}{n_e^2} \right]^{-\frac{1}{2}} \right\}, \quad (3)$$

By rotating the magnet assembly while keeping the sample stationary, we only change  $n_d$  without affecting the polarization direction of the THz wave. The maximum magnetic inclination angle is  $55^\circ$ . Beyond that, the THz beam would be blocked by the magnet in the current experimental setup.

Spectral transmittance of the 2D-MHA is measured by using a photoconductive-antenna-based THz time-domain spectrometer (THz-TDS) [27]. The size of the 2D-MHA (about 250 holes in the aperture) is large enough to avoid the finite size effect [28]. The finite time extent of the terahertz pulse scans, 136 ps (in 1024 steps), limits the frequency resolution of the numerical Fourier transforms in THz-TDS. To perform a numerical interpolation between the measured frequency points, the measured pulses in the time domain were extended with zeros (zero padding) [15] to a total time duration of 1500 ps.

### 3. Results and discussion

Figure 2 shows the measured zeroth-order transmission spectra for the 2D-MHA in several configurations.

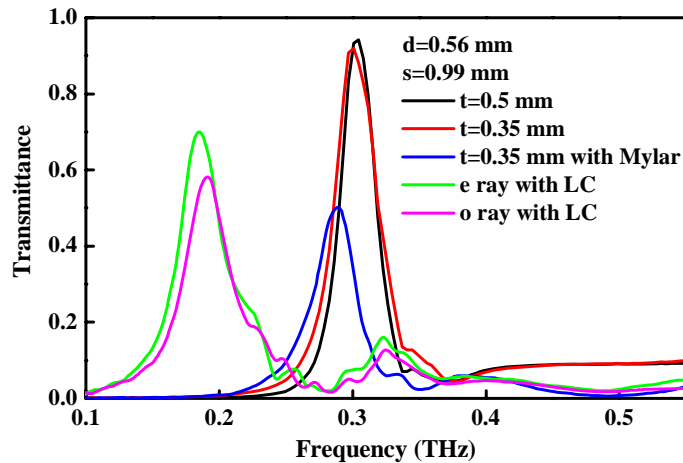


Fig. 2. Transmittance of the 2D-MHA sample before machining (thickness  $t = 0.5$  mm, black trace), after machining into a box-line structure ( $t = 0.35$  mm, red trace), boxed MHA with front and back Mylar sheets attached (blue trace), LC-filled MHA for o-ray (purple trace) and LC-filled MHA for e-ray (green trace).

The band-pass transmission peak for the 2D-MHA sample before machining (black trace) is observed at 0.304 THz. The peak transmission is close to unity, which is about 3 times higher than the value 0.29 expected from the porosity of the 2D-MHA. This transmission peak frequency is close to the resonant frequency of the SPP (0.349 THz) on a smooth surface and does not change appreciably after it was machined into the box-like structure (red trace). With front and back Mylar ( $n = 1.70$ , independently measured in our lab) sheets attached (blue trace), the peak frequency red-shifted to 0.289 THz, while the cutoff behavior remains unchanged. The peak transmittance also reduces appreciably from 0.92 to 0.50. In this case, the peak frequency of the 2D-MHA is located below the cutoff frequency. As a result, the extinction coefficient of the waveguide mode becomes large as the resonant frequency of the SPP shifts to the lower frequency due to the dielectric substrate while  $\nu_c$  remains unchanged. Consequently the peak transmittance significantly decreases [13]. The other possible mechanism is the decrease of the resonance effect between the SPP on the two sides of the metal slab, dielectric and air [29].

The frequencies of the main transmission peaks of LC-filled 2D-MHA for o-ray ( $\vec{B} // \hat{z}$ , purple trace in Fig. 2) and e-ray ( $\vec{B} // \hat{y}$ , green trace in Fig. 2), i.e., 5CB aligned perpendicular and parallel to the polarization of the incident THz wave, respectively, are red-shifted further to 0.193 THz and 0.188 THz. Using the indices of refraction of 5CB ( $n_o = 1.57$  and  $n_e = 1.75$ ) and expressions for the cutoff and diffraction frequencies presented earlier, we estimate that  $\nu_c = 0.200$ ,  $\nu_{\text{diff}} = 0.222$  and  $\nu_R = 0.191$  THz for the perpendicular geometry (o-ray). Similarly,  $\nu_c = 0.179$  THz,  $\nu_{\text{diff}} = 0.199$  THz and  $\nu_R = 0.171$  THz for the parallel geometry (e-ray). Thus the observed peak transmission frequencies are close to that of the theoretical estimates.

As we change from the perpendicular (o-ray) to the parallel (e-ray) geometry, the peak transmission (see Fig. 2) increases from 0.58 to 0.70. As a THz wave filter, the insertion loss of the present device is thus 2.35 to 1.55 dB, while the quality factors or Q-factors are between 4 and 5. For both geometries, the transmittance is larger than that of the device before filling with LC, 0.50. This can be qualitatively understood by noting that, while the resonance frequencies of the MHA-LC structures red-shifted to 0.191-0.171 THz, the cutoff frequency also shifted to a lower frequency of 0.2-0.179 THz from 0.314 THz for the bare

2D-MHA because a dielectric, LC is filled in the holes. Considering the porosity of the tunable 2D-MHA, 0.29, we observe an enhancement factor of 2.42.

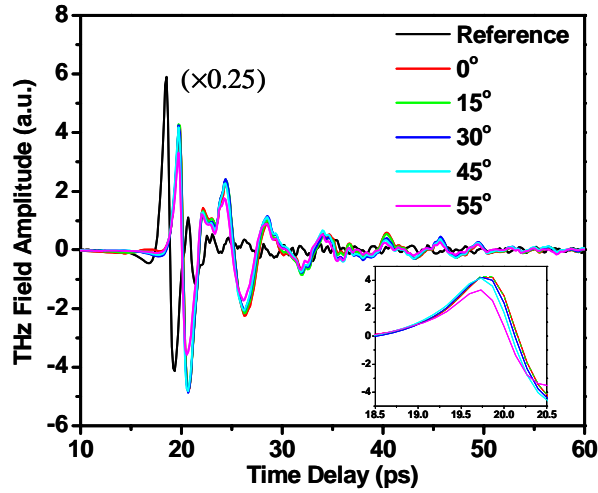


Fig. 3. The transmitted THz temporal waveforms of the tunable 2D-MHA sample with the 5CB layer aligned at several magnetic inclination angles  $\theta$  ( $\theta = 0^\circ, 15^\circ, 30^\circ, 45^\circ$  and  $55^\circ$ ) to the polarization direction of the THz wave. The relative time delay is clearly shown in the inset. The waveform of the incident or reference THz pulse (reduced by a factor of four) is also shown.

The temporal waveforms of the THz pulse transmitted through the tunable 2D-MHA sample with the 5CB layer aligned at several magnetic inclination angles  $\theta$  ( $\theta = 0^\circ, 15^\circ, 30^\circ, 45^\circ, 55^\circ$ ) are shown together with that of the incident or reference THz pulse (reduced by a factor of four for it to be shown on the same graph) in Fig. 3 above. The transmitted THz waves for larger  $\theta$  exhibit smaller time delay relative to that of the reference (see the inset), because the effective refractive index of 5CB reduces with increasing  $\theta$ .

A close-up view of the power spectra of THz signals transmitted through this device at various magnetic inclination angles are shown in Fig. 4. The changes in peak frequency and height with  $\theta$ , or the effective index of refraction of the LC, are evident.

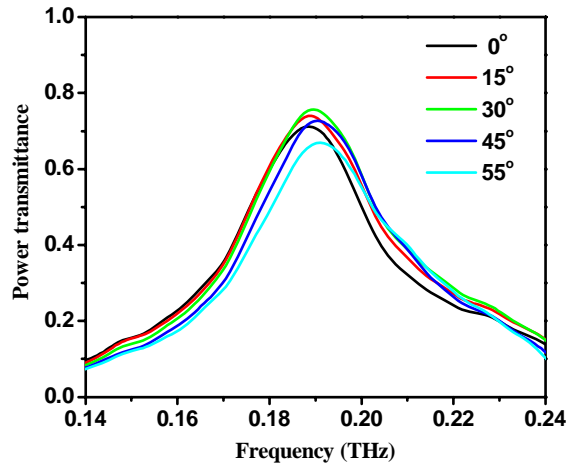


Fig. 4. A close-up of the power spectra of THz signals transmitted through this device at various magnetic inclination angles.

We also plotted experimentally observed shifts of the peak transmission frequencies from those of the Mylar-packaged and boxed 2D-MHA before filling with LC as a function of the inverse of the effective index of refraction,  $1/n_{\text{eff}}$ , in Fig. 5.

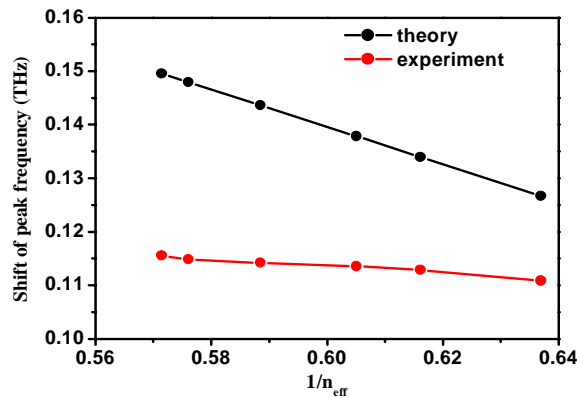


Fig. 5. The experimentally observed shift of the peak frequencies from Fig. 3(a) and the theoretical estimates are plotted as a function of the inverse of the effective index of refraction.

The experimentally obtained tuning range is 0.0047 THz as we vary  $\theta$  from  $0^\circ$  to  $90^\circ$ . An estimate of the potential tuning range of the device can be deduced from Eq. (2),  $|\Delta\nu_R| \sim \Delta n_d v_{\text{spp}} / n_d^2$ , where  $v_{\text{spp}}$  is the resonance frequency of the device before filling with LC. For the ideal case, if the substrate is infinite, the maximum tuning range using 5CB should then be  $\sim 0.02$  THz. Experimentally, several of the authors have previously shown that the frequency shift can be increased by using matching dielectric substrates on both side of the 2D-MHA [29]. This is expected to be the case for the current device with LC also. Further, highly anisotropic LC with birefringence as high as 0.37 (versus  $\sim 0.2$  for 5CB) at microwave frequencies has been reported for a special mixture from Merck [30]. With the use of such LC, we can expect the tuning range extending to  $\sim 0.037$  THz.



The shifts according to the theoretical estimates using Eq. (2),  $|v_R - v_{\text{diff}}| = v_{\text{diff}} |(1/n_d) - 1|$ , are also shown in the same figure. General linear trends with  $1/n_d$  are observed for both. There is, however, significant discrepancy in the slopes of the two. Qualitatively, this can be understood by noting that the theoretical model assumes an infinite dielectric substrate. Experimentally, the liquid crystal “substrate” is of finite thickness. Further, Eq. (1) does not take into account effect of filling of the holes with LC instead of air. It could be argued that it is not necessary to invoke SPPs in order to explain the measurements, as the cutoff frequency also varies with the index of refraction of the LC in the holes. The transmission peak frequency, however, does not necessarily change with the cut-off frequency. Previously, we have measured the zero-order transmission spectra of the 2D-MHA by changing the thickness of the dielectric (polymer) layer [29] and found that the band-pass transmission peak shifts to the lower frequency side with increasing the layer thickness, even though the cutoff frequency does not change (the material filling the holes were air always in that experiment). We note that the error in the measurement of the peak positions is  $\sim 0.0007$  THz, much smaller than the shift we detected, 0.0047 THz. Because the SPP resonance frequencies and the cutoff frequencies are very close in the present experiment, however, we cannot rule out completely the possibility that the peaks could be guided modes in the holes.

The change in peak transmittance of the 2D-MHA by varying the effective index of refraction of the LC is shown in Fig. 6. The THz transmission peak increases with  $\theta$  for  $\theta < 30^\circ$ . This can be explained by how close the refractive index of LC matches that of Mylar. The ordinary and extraordinary refractive indices of 5CB are 1.57 and 1.75, respectively, at 0.3 THz. With increasing  $\theta$ , the effective refractive index of LC will descend from 1.75 to 1.70 (from  $\theta = 0^\circ$  to  $\theta = 30^\circ$ ) and the refractive index of Mylar substrate, which is 1.70. Over  $30^\circ$ ,  $n_d$  will decrease from 1.70 to 1.57 with increasing  $\theta$ . The transmission peak will then decrease according to the same theory.

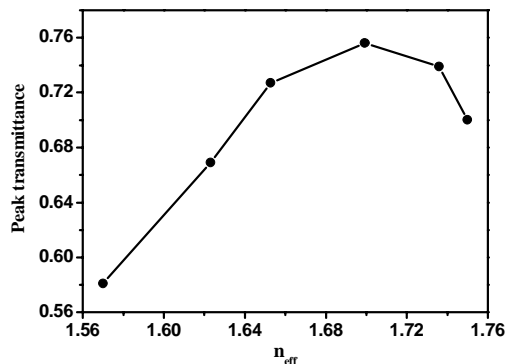


Fig.6. The peak transmittance of the 2D-MHA is plotted as a function of the inverse of the effective index of refraction of the LC.

It is interesting to compare our present results with that of Kim *et al.* [11], who modulated the transmission amplitude (by 25%) in the near IR of a perforated metal film–liquid crystal–indium tin oxide cell by varying the voltage applied to the LC. The thickness of the LC was 10 microns. At THz frequencies, the thickness of the LC must be of the order of wavelength or longer, i.e., several hundred microns in order to achieve significant frequency-tuning effect. For such a thick LC cell, it is difficult to align. Thus we employ a relatively strong permanent magnet ( $\sim 0.15$  T). Tuning is achieved by varying the magnetic field. On the other hand, the spectral shift in the data of Kim *et al.* [11] is not immediately apparent, because the spectral features were quite broad in that experiment. Frequency tuning is clearly demonstrated in the present work. The dynamics of the nematic liquid cell (without external biasing field) is

determined by its boundary condition. For our device with LC thickness and the metallic hole array with hole diameters both of the order of wavelength,  $\sim 0.5$  mm, the relaxation time is  $\sim 250$  s. We use magnetic field tuning, however. With a magnetic field (0.15 T) 40 times higher than that of the threshold field ( $\sim 0.05$  T), the relaxation time (both rise and fall) reduces by a factor of  $\sim (40)^2$  to 0.15 s. Although the present device is not suitable for fast switching and modulation because the switching time of LC is quite long, it would be ideal for application such as tunable filtering and could be a prototype for a highly sensitive THz sensor as the peak transmission frequency of the device is sensitive to the optical constant of the dielectric, e.g., liquid crystal.

#### **4. Conclusions**

In summary, we demonstrate frequency tuning of enhanced THz radiation transmitted through a two-dimensional metallic hole array (2D-MHA) by controlling the index of refraction of the medium filling the holes and adjacent to the 2D-MHA on one side. The medium is a nematic liquid crystal (NLC) 5CB and its index of refraction is varied using the dependence of the effective index of refraction of the NLC on the magnetic field. With the NLC, the peak transmission frequency of the 2D-MHA shifts to the red by 0.112 THz and can be tuned between 0.193 and 0.188 THz. The maximum transmission of the device is well above (2.42 times) that according to the fractional area occupied by the holes and varies from 55% to above 70%. As a filter, the present device exhibits a continuous tuning range of 4.5 GHz, relatively low insertion losses of 2.35 to 1.55 dB and a Q-factor of  $\sim 4$ -5. The tuning range can be as high as 0.037 THz by employing matching LC substrates on both sides of the 2D-MHA and highly anisotropic LC materials. The Q-factor can be improved by cascading two or more such filters.

#### **Acknowledgments**

Most of this work was performed while Ci-Ling Pan was on sabbatical and Cho-Fan Hsieh was a research student at Osaka University. Additional support of Ci-Ling Pan by the National Science Council of R.O.C. is also gratefully acknowledged.